Bubble oscillations in the nearly adiabatic limit

V. Kamath, H. N. Oğuz, and A. Prosperetti
Department of Mechanical Engineering, The Johns Hopkins University, Baltimore, Maryland 21218

(Received 6 January 1992; accepted for publication 2 June 1992)

Miksis and Ting [J. Acoust. Soc. Am. **81**, 1331 (1987)] reported examples of a marked increase of the radius of an oscillating gas bubble as predicted by their nearly adiabatic model. They attributed this phenomenon to a process of rectified heat transfer into the bubble. By comparison with a more complete model which contains the nearly adiabatic one as an approximation, it is shown that the real cause of this result is instead the error inherent in the approximation. This error arises primarily from the failure of the approximation to capture the complex behavior of the gas temperature and manifests itself in a spurious growth of the mass of gas contained in the bubble. In addition to being more accurate, the more complete model is also found to be less computationally demanding than the approximate one.

PACS numbers: 43.35.Ei

INTRODUCTION

In two interesting papers[1,2] Miksis and Ting studied the forced sinusoidal oscillations of a gas bubble of radius much greater than the thermal penetration length in the gas. On the basis of the assumption that, in this limit, the gas behaves nearly adiabatically, they were able to obtain an integral equation of the Volterra type for the gas pressure.[1] In a numerical study of this model, they reported the unexpected finding that, in certain conditions, the time-averaged radius of the oscillating bubble could become substantially larger than its static value.[2] This result was puzzling and the attempt to understand it better has motivated the present work.

Our conclusion is that the radius increase reported by Miksis and Ting arises in reality from the inaccuracy of the nearly adiabatic approximation which manifests itself in a spurious increase of the mass of gas contained in the bubble. This result has been mentioned in a recent paper[3] in which however Miksis and Ting's numerical method was erroneously questioned. Here, we present a fuller discussion.

The above conclusion is supported by two arguments. In earlier papers[3–5] we have derived a comprehensive model of the thermo-fluid mechanical behavior of the gas contained in a spherical bubble. Under the same assumption of near adiabaticity used by Miksis and Ting, it has been shown that their result follows from this complete model,[3] which is therefore useful to judge the accuracy of the approximation. We find that, already at the beginning of the second or third cycle, the results of the approximate and of the complete models start diverging substantially. A second test, "internal" to the quasiadiabatic approximation in that it does not rely on comparisons with other models, consists in checking the satisfaction of a lower bound for the mass of gas contained in the bubble. This bound is computable within the framework of the quasiadiabatic approximation and is found to be grossly exceeded.

The point of course is not that the results of Ref. 1 are incorrect. They are the fruit of a correct analysis and can, in fact, be checked by an alternative derivation.[3] Rather, we find that the residual error converges to zero too slowly for practical applications. The result, therefore, while conceptually quite interesting in showing explicitly the effects of the system's memory, appears to be of limited use.

I. MATHEMATICAL MODELS

Following Refs. 1 and 2, in the description of the radial dynamics of the oscillating bubble, we ignore the compressibility of the liquid and use the Rayleigh–Plesset equation

$$R\frac{d^2R}{dt^2}+\frac{3}{2}\left(\frac{dR}{dt}\right)^2 = \frac{1}{\rho}\left(p(t)-p_\infty(t)-2\frac{\sigma}{R}-4\frac{\mu}{R}\frac{dR}{dt}\right), \tag{1}$$

where $R(t)$ is the instantaneous radius of the bubble at the time t, $p(t)$ is the internal gas pressure, σ is the interfacial tension, ρ is the liquid density, and μ is its viscosity. The time-varying external pressure $p_\infty(t)$ that drives the oscillations is taken to be

$$p_\infty(t)=P_0(1-\epsilon\sin\omega t), \tag{2}$$

where P_0 is the static pressure, ω is the angular frequency, and ϵ is the dimensionless forcing amplitude.

In the comprehensive model of Refs. 3–5, the internal pressure p is obtained from the solution of the gas energy equation incorporating a special explicit expression for the local gas velocity. Underlying this expression are the assumptions (also made by Miksis and Ting in Ref. 1) of the spatial uniformity of the gas pressure and the perfect nature of the gas. In view of the rather complex form of the equations of this complete model we do not reproduce them here and refer the reader to the original papers. Suffice it to say that the version of this complete model used here exactly adheres to Miksis and Ting's work and furnishes therefore a legitimate basis for comparison. In particular, the proportionality between thermal conductivity and temperature used by them is also adopted.

Following Miksis and Ting, in nearly adiabatic conditions, one may postulate the presence of a thermal boundary

layer adjacent to the bubble surface, and an approximate asymptotic solution of the gas energy equation becomes then possible. In this way, the following integral equation for the gas pressure can be obtained[3]

$$p_* R_*^{3\gamma} = 1 + \frac{3\gamma}{4\pi}\left(\frac{D}{\pi}\right)^{1/2} \times \int_0^{\theta_*} [p_*^{-(\gamma-1)/\gamma}(\theta_* - \eta_*) - 1]\eta_*^{-1/2}\, d\eta_*, \tag{3}$$

where γ is the ratio of the gas specific heats and

$$\theta_* = (4\pi)^2 \int_0^{t_*} p_*(t'_*) R_*^4(t'_*)\, dt'_*. \tag{4}$$

These equations are written in dimensionless variables, denoted by asterisks, to render explicit the appearance of the small perturbation parameter

$$D = \chi/\omega R_0^2 \ll 1, \tag{5}$$

(where χ is the thermal diffusivity of the gas) measuring the thickness of the thermal boundary layer with respect to the equilibrium radius of the bubble R_0. The other quantities appearing in Eqs. (3) and (4) are defined by

$$p_* = p/p_0, \quad R_* = R/R_0, \quad t_* = \omega t, \tag{6}$$

where $p_0 = P_0 + 2\sigma/R_0$ is the internal gas pressure at equilibrium. In place of (3) Miksis and Ting give the expression[1]

$$p_*^{1/\gamma} R_*^3 = 1 + \frac{3}{4\pi}\left(\frac{D}{\pi}\right)^{1/2} \times \int_0^{\theta_*} [p_*^{-(\gamma-1)/\gamma}(\theta_* - \eta_*) - 1]\eta_*^{-1/2}\, d\eta_*, \tag{7}$$

which is evidently equivalent to first order in D. In the following, we shall use this equation to calculate p_*. The results deriving from Eq. (3) will be considered at the end.

II. NUMERICAL METHOD

A pseudospectral method, discussed in detail in Ref. 5, is used for the numerical solution of the complete model. Its accuracy can be monitored during the numerical integration by calculating, from the computed temperature field and pressure, the total gas mass within the bubble. In our previous studies,[4,5] this quantity has proven to be a reliable indicator of the accuracy of the calculation. In all the cases considered for the present study, the mass anomaly was never found to exceed 0.5%.

To evaluate the convolution integral in (3) or (7), we divide the integration range into two parts. The contribution of the first part is evaluated by the trapezoidal rule using values of p stored at equally spaced times. The second part, which consists of the last computed six time steps, is handled in a special way because of the square-root singularity. First, a cubic spline is fitted to the term in brackets in the integrand of Eq. (7) [or (3)] so that its value can be computed at any point by interpolation. Then, with this approximation, an adaptive Gaussian quadrature (QUADPACK routine qaws) with a weighting factor of $s_*^{-1/2}$ is employed to efficiently account for the singularity. The final step of evaluating the pressure at the new time level requires iteration because of the implicitness of these formulas. A good initial guess is available from the value at the previous time step since the correction is small by hypothesis. Typically, less than 10 iterations are sufficient for convergence to within 10^{-2}% of the final value. We have decreased the tolerance to 10^{-3}% and 10^{-4}% with negligible effects on the results. The number of points used for the pressure interpolation, 200 per cycle, was sufficiently large that linear interpolation in place of cubic splines introduced negligible differences. A coarser discretization with 100 points per cycle also only had minimal effects.

The numerical approach taken for the solution of the system formed by the radial equation (1) and the integral equation (7) is based on Gear's stiff integration technique and the globally adaptive integration scheme of Piessens *et al.*, respectively, as implemented in the IMSL's routine ivpag.[6,7] Clearly, the computation of the convolution integral becomes more and more time consuming as the simulation progresses.

III. RESULTS

In Ref. 2, Miksis and Ting present numerical results for a 100-μm radius air ($\gamma = 1.4$) bubble in water at 20 °C and 1-atm pressure. They calculate the resonance frequency from the purely adiabatic relation

$$\omega_0^2 = \frac{3\gamma p_0}{\rho R_0^2}\left(1 - \frac{2\sigma}{R_0 p_0}\right), \tag{8}$$

although the natural frequency computed from their model is actually given by[3]

$$\omega_0^2 = \frac{3\gamma p_0}{\rho R_0^2}\left(1 - \frac{2\sigma}{R_0 p_0} - 3(\gamma-1)\sqrt{\frac{D}{2}}\right). \tag{9}$$

So as to consider exactly the same cases studied by them, we shall neglect the $O(\sqrt{D})$ correction in this relation and use (8) to calculate ω_0 and find $\omega_0/2\pi = 32.8$ kHz for $R_0 = 100$ μm. They consider excitation of the bubble at frequencies $\omega/\omega_0 = 0.55$, 1.0, and 2.0 and dimensionless forcings $\epsilon = 0.5$ and 0.75. We have repeated all their calculations but present results only for the most interesting ones.

Typical of the unexpected findings that they describe is the case $\omega/\omega_0 = 0.55$, for which $D = 0.0176$, $D^{1/2} = 0.133$, with a dimensionless forcing pressure amplitude $\epsilon = 0.75$. They report that "After passage through a very large amplitude region the oscillations appear to settle down to a periodic oscillation about a larger mean radius." From their Fig. 7, it can be seen that, after a few oscillations, the radius-time curve loses the prominent harmonic component at 2ω initially present. At the same time, the average radius increases and, after a period of violent oscillations, eventually appears to stabilize around $R/R_0 \simeq 2$. The oscillations, although strongly nonlinear, appear to be synchronous with the forcing as if the bubble were driven close to the fundamental resonance rather than the first harmonic resonance. Due to the inverse proportionality of natural frequency and radius,

for a fixed value of ω, a doubling of the radius would halve ω_0, thereby indeed bringing the forcing close to resonant conditions. A similar behavior was found for the same frequency and the weaker forcing $\epsilon = 0.5$.

In Fig. 1, we plot for this case ($\omega/\omega_0 = 0.55$, $\epsilon = 0.75$) the nondimensional radius of the bubble starting from rest as computed by us. Following Miksis and Ting, the abscissa in this and the following figures is the dimensional time t divided by the characteristic time

$$\tau = R_0\sqrt{\rho/P_0}\,. \tag{10}$$

For the examples given in this paper $\tau = 9.99\,\mu$s. In this unit the (dimensionless) period of the forcing is $\omega\tau/2\pi = 5.54$. Figure 1(a) shows the motion during the first 36 periods of the forcing pressure field and Fig. 1(b) from the 81st to the 100th period. The results of the complete model are shown by the solid line while the dashed line is for the nearly adiabatic approximation (7). The two curves are close for the first two cycles, but substantial differences unfold as the integration progresses. For example, it is clear from Fig. 1(b) that the complete model predicts the motion to settle down to a regime of steady oscillation with an appreciable component at 2ω and a relatively small amplitude. The approximate model, on the other hand, indicates a gradual loss of the harmonic component and a rapid growth of the oscillation amplitude in the course of the 19th–21st period just as in Miksis and Ting's calculation. This evolution can be appreciated even more clearly from Fig. 2, where the running average of the radius $\bar{R}(t)$ is shown for the first 100 cycles. All these results are identical to those of Miksis and Ting. The same behavior was found at the lower amplitude $\epsilon = 0.5$ with the complete model showing a steady state with a strong harmonic component.

Another example with $\omega/\omega_0 = 1.0$ ($D = 0.00970$, $D^{1/2} = 0.0985$, $\omega\tau/2\pi = 3.05$) and $\epsilon = 0.75$ is illustrated in Figs. 3 and 4. Part (a) of the first figure shows the radius versus time during the periods 1 to 16 of the driving, while part (b) is for the periods 82 to 100. As before, the solid line shows the results of the complete model and the dotted line those of the quasiadiabatic approximation. Figure 4 is analogous to Fig. 2 and shows $\bar{R}(t)$ for the first 100 periods. Even though the oscillation amplitudes in this case are greater than those of Fig. 1(a), as found by Miksis and Ting, no strong transition is encountered. However, it is clear that the radius-time curve predicted th the approximation is significantly different from that of the complete model.

The divergence of the nearly adiabatic approximation from the complete model from which it derives is clearly illustrated by these comparisons.

We have also compared the two models in the first subharmonic region. The qualitative behavior of the nearly adiabatic one is unchanged except for a smaller rate of error accumulation due to the reduced oscillation amplitude.

IV. DISCUSSION

It is well known that an oscillating bubble is a "softening" nonlinear oscillator in the sense that, in an amplitude-versus-frequency diagram, the resonant peaks lean toward lower frequencies.[4,8,9] Hence if, in the course of the oscillations, the ratio ω/ω_0 is made to slowly increase from a small value, at some sharply defined points,[9] the motion will be attracted by a series of resonances with a strong transient and a considerable increase in amplitude as in Fig. 1. On the other hand, a radius increase starting from $\omega/\omega_0 = 1$ will

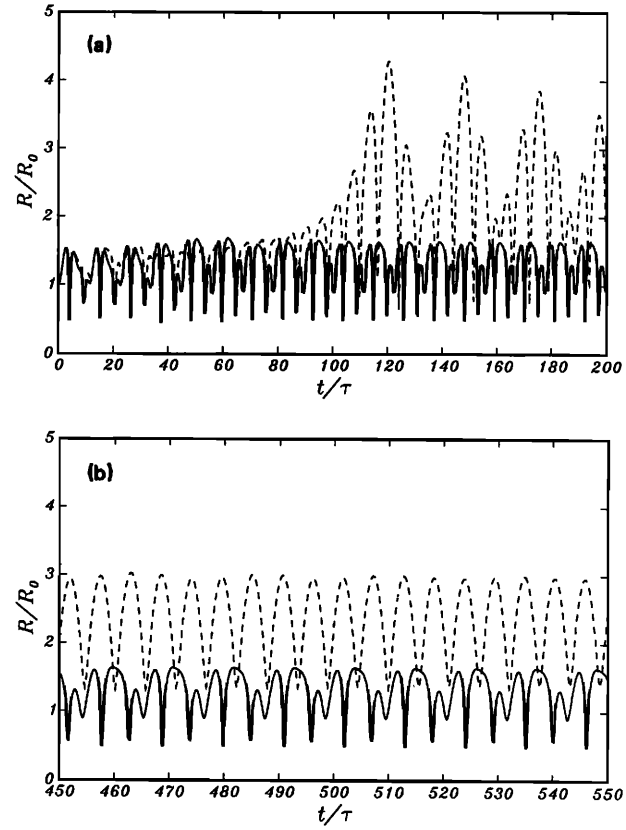

FIG. 1. Comparison between the radius-time behavior predicted by the complete model (solid line) and the nearly adiabatic approximation (7) (dotted line) for $\omega/\omega_0 = 0.55$, $\epsilon = 0.75$, $R_0 = 0.1$ mm. The physical properties are those of air and water at normal temperature and pressure. The characteristic time unit τ, defined in Eq. (10), has the value $\tau = 9.99\,\mu$s. The dimensionless period of the forcing is $\omega\tau/2\pi = 5.54$. (a) The motion during the first 36 periods of the forcing and (b) the motion during the periods 81 to 100.

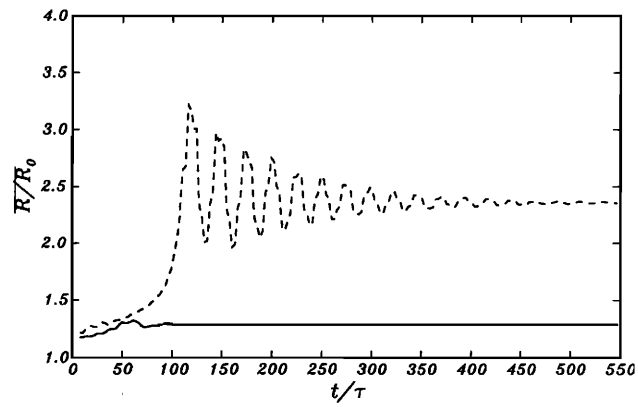

FIG. 2. Running average of the bubble radius versus time for the same case as in the previous figure according to the complete model (solid line) and the nearly adiabatic approximation (dotted line) for the first 100 cycles of the forcing.

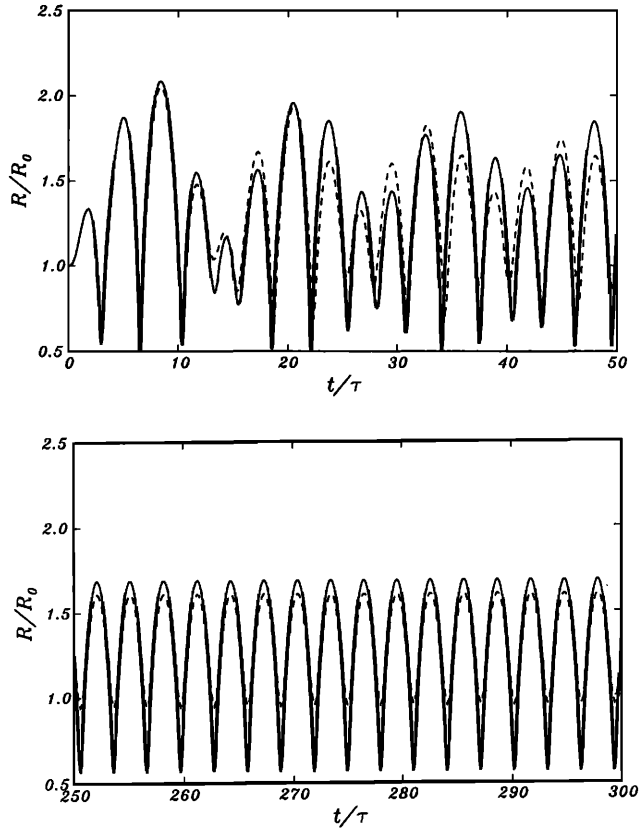

FIG. 3. Comparison between the radius-time behavior predicted by the complete model (solid line) and the nearly adiabatic approximation (7) (dotted line) for $\omega/\omega_0 = 1$, $\epsilon = 0.75$, $R_0 = 0.1$ mm. The physical properties are those of air and water at normal temperature and pressure. The characteristic time unit τ, defined in Eq. (10), has the value $\tau = 9.99\ \mu$s. The dimensionless period of the forcing is $\omega\tau/2\pi = 3.05$. (a) The motion during the first 16 periods of the forcing and (b) the motion during the periods 82 to 100.

result in a decrease of the oscillation amplitude as the descending portion of the resonant peak is gradually described, in qualitative agreement with Fig. 3.

Miksis and Ting attribute the increase of the effective bubble radius to rectified diffusion of heat, a process that is well known to occur in the case of oscillating vapor bubbles (see, e.g., Refs. 10–13). We will show that this effect, while present, is however small and quite insufficient to account for their findings. Rather, these derive from an accumulation of the error introduced by the quasiadiabatic approximation which is equivalent to a spurious increase of the mass m of gas contained in the bubble as suggested in Ref. 3. (Energy, on the other hand, is conserved exactly.) The approximation fails therefore to be uniformly valid in time. This conclusion can easily be established as follows. In view of the assumed perfect nature of the gas, the total mass contained in the bubble can be computed from

$$m_* \equiv \frac{m}{m_0} = 3p_* R_*^3 \int_0^1 \frac{T_0}{T(y,t)} y^2\, dy = 1, \tag{11}$$

where m_0 is the initial mass, T the local gas temperature, T_0 the initial (uniform) gas temperature, and $y = r/R(t)$. The quasiadiabatic approximation is derived assuming that the instantaneous temperature distribution in the gas consists of a "core" very close to the adiabatic value

$$T_{\rm ad}/T_0 = p_*^{(\gamma-1)/\gamma} \tag{12}$$

and a thin boundary layer across which the temperature falls monotonically to the undisturbed value at $r = R(t)$. If (12) is used to calculate the integral in (11), one finds

$$m_{\rm ad} = p_*^{1/\gamma} R_*^3. \tag{13}$$

Near radius minima the bubble core is hot and, if the temperature distribution is as described above, one concludes that $T \leqslant T_{\rm ad}$ throughout the bubble. It follows therefore that in this situation (13) should underestimate the value of the integral in (11) so that

$$m_{\rm ad} \leqslant 1 \quad \text{near radius minima.} \tag{14}$$

We show in Fig. 5 a graph of $m_{\rm ad}$ for the first 36 cycles of the case of Fig. 1 for the nearly adiabatic approximation (upper curve) and for the complete model (lower curve). In view of the fact that $m_{\rm ad}$ acts as a lower bound only in the

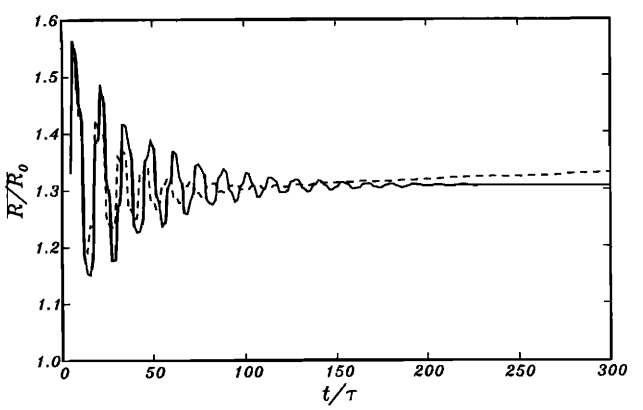

FIG. 4. Running average of the bubble radius versus time for the same case as in the previous figure according to the complete model (solid line) and the nearly adiabatic approximation (dotted line) for the first 100 periods of the forcing.

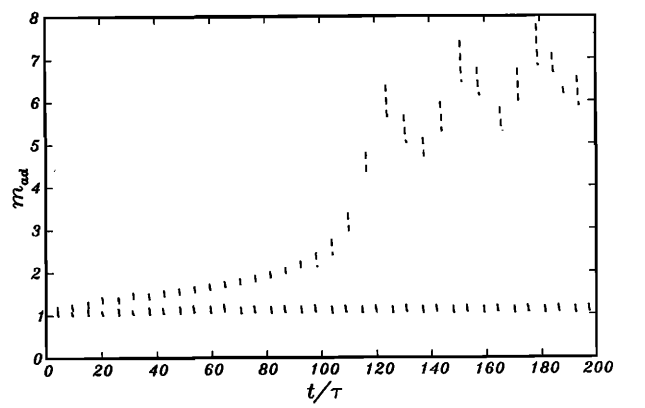

FIG. 5. Graph of the quantity $m_{\rm ad}$ defined in Eq. (13) as given by the complete model (lower curve) and by the quasiadiabatic approximation (upper curve, dashed) during the first 36 cycles of the forcing for the case of Figs. 1 and 2. Since this quantity acts as a lower bound for the mass of gas contained in the bubble only near the radius minima, it is plotted only during the time intervals when $p_* > 2$. For the mass to be conserved, if the adiabatic approximation were valid, $m_{\rm ad}$ should stay below 1. See text.

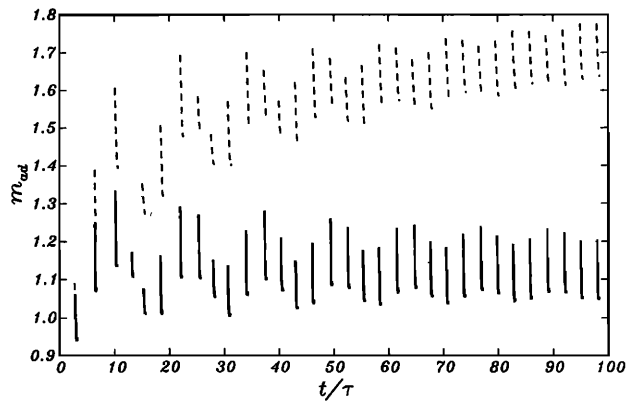

FIG. 6. Graph of the quantity m_{ad} defined in Eq. (13) as given by the complete model (lower curve) and by the quasiadiabatic approximation (upper curve, dashed) during the first 33 cycles of the forcing for the case of Figs. 3 and 4. Since this quantity acts as a lower bound for the mass of gas contained in the bubble only near the radius minima, it is plotted only during the time intervals when $p_* > 2$. For the mass to be conserved, if the adiabatic approximation were valid, m_{ad} should stay below 1. See text.

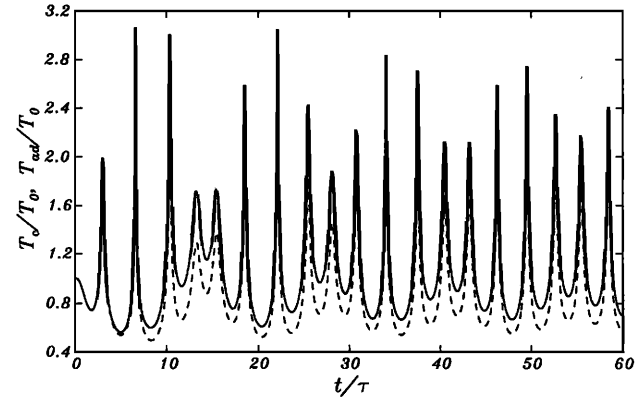

FIG. 8. The solid line shows the dimensionless temperature T_c/T_0 at the center of the bubble as calculated from the complete model for the first 20 cycles of the case of Figs. 3 and 4. The dotted line is the adiabatic temperature given by Eq. (12) computed from the value of p_* also obtained from the complete model.

neighborhood of the radius minima, we show this quantity only during the time intervals such that the pressure of the gas in the bubble is greater than twice the equilibrium value to guarantee that the bubble is indeed collapsing. (Since the average radius is growing according to the approximation, a criterion based on this variable would not be suitable to identify the collapse phases.) It is apparent that, while in the early part of the calculation m_{ad} as computed from the nearly adiabatic approximation slightly exceeds 1, as the integration progresses it rapidly grows to values well above 1. As a matter of fact, it is found that, in the range shown in Fig. 1(b), m_{ad} oscillates around a value close to 8, consistent with a doubling of the bubble radius. Similar results for the case of Figs. 3 and 4 are presented in Fig. 6, and again the bound (14) is seen to be conspicuously violated by the approximation, although by not nearly as much as in the previous case. The same behavior is found in all the other cases considered by Miksis and Ting. For example, for $\omega/\omega_0 = 1$ (the case of Figs. 3 and 4) even at the low forcing $\epsilon = 0.2$, we find values of the order of 1.15 for m_{ad} after 15–20 cycles.

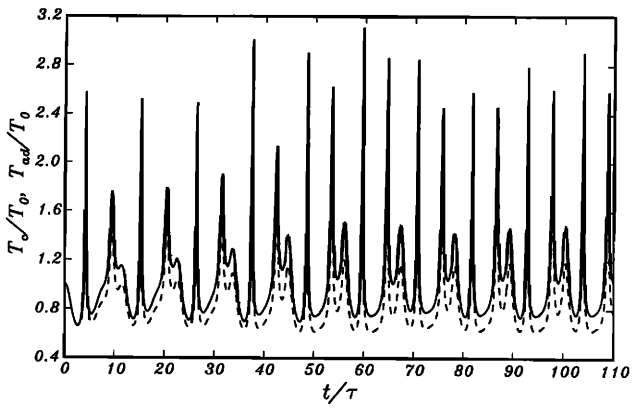

FIG. 7. The solid line shows the dimensionless temperature T_c/T_0 at the center of the bubble as calculated from the complete model for the first 20 cycles of the case of Figs. 1 and 2. The dotted line is the adiabatic temperature given by Eq. (12) computed from the value of p_* also obtained from the complete model. Note that the bubble center becomes hotter than the adiabatic estimate after the first cycle.

It is seen in Figs. 5 and 6 that, although much better behaved, the value of m_{ad} given by the complete model also shows a tendency to have minimum values slightly above 1 after a few cycles. As mentioned before, we have checked directly the value of the integral (11) in the complete model and we have consistently found errors smaller than 1% even after hundreds of cycles. The explanation of the phenomenon is therefore different, and can be understood from Figs. 7 and 8 which show, for the complete model, the actual computed temperature T_c at the bubble center (solid line) and the adiabatic value (12) (dotted line). It is clear that, while the two curves coincide up to the first bubble collapse, the adiabatic temperature remains thereafter slightly *below* the actual temperature. Therefore, since T_{ad}, although close to the center temperature, is slightly smaller, the quantity m_{ad} fails to be an exact lower bound for the mass by a few percent. It is clear that this circumstance in no way affects our conclusions on the failure of mass conservation in the nearly adiabatic approximation. In the first place, the effect is small (as can be judged from the results of the complete model), while m_{ad} as given by the approximation far exceeds the error arising from the use of a sightly incorrect core temperature. Second, as remarked above, the assumption that, during the collapse phase, $T \leqslant T_{ad}$, is inherent in the approximation, and if this inequality is incorrect, so is the approximation itself.

At first sight the fact that the core temperature is greater than T_{ad} is rather surprising. We have already encountered this behavior in Ref. 14, where we have offered an explanation that basically coincides with Miksis and Ting's rectified diffusion of heat. As is clear from Figs. 1 and 3, bubble oscillations are characterized by a marked asymmetry between the expansion and collapse phases with the former much longer than the latter. When the bubble expands past its equilibrium radius, it tends to cool with respect to the surrounding liquid and therefore heat is conducted into the gas. The contraction phase is much shorter and, although the gas

is now hotter than the liquid, the energy lost by conduction is less than that acquired during the preceding expansion. This process is enhanced by the spherical geometry which causes different thicknesses of the liquid thermal boundary layer in the two phases, just as in the case of rectified mass diffusion.[15] This effect of rectified heat transfer is however clearly seen from our results to have a rather modest magnitude. Indeed, only a slight increase in the average gas temperature is sufficient to offset the bias in the collapsing versus the expanding phase heat exchanges as can be judged from the fact that the oscillations quickly become steady, as shown in Figs. 1 and 3. On a much longer time scale, a second and more significant rectified heat transfer process takes place. As the liquid surrounding the bubble gradually heats up, the temperature of the gas also needs to increase according to the same mechanism outlined above and this process can continue basically indefinitely. We have carried out some preliminary calculations that will be reported in due course and find that time scales of the order of thousands of cycles are necessary to obtain a barely detectable effect. In any event, this process cannot be studied with either one of the models used here which both assume that the heat capacity of the liquid is essentially infinite.

To gain a better understanding of the reasons for the failure of the nearly adiabatic approximation, it is interesting to show the evolution in time and space of the gas temperature, which we do in Figs. 9 to 12. Here the temperature calculated from the complete model is divided by the adiabatic value (12) before plotting to bring out more vividly the discrepancy between the actual temperature behavior and that assumed in the derivation of the approximation. Figures 9 and 10 are three-dimensional graphs showing T/T_{ad} as a function of both $r/R(t)$ and time for the first 5 cycles of the cases with $\omega/\omega_0 = 0.55$ and 1 studied before. It is clear that T/T_{ad} very quickly becomes appreciably different from 1 essentially everywhere. Indications of a nonmonotonic behavior of the temperature field are also present. To explore this feature, we show in Figs. 11 and 12 sequences of temperature distributions at different instants during the first three cycles of the previous examples. The picture is quite

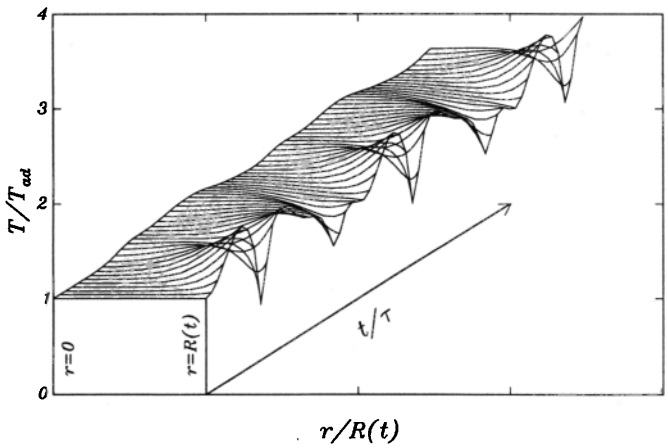

FIG. 9. Space-time plot of the gas temperature divided by the adiabatic value (12) during the first five cycles of the case $\omega/\omega_0 = 0.55$ of Figs. 1 and 2.

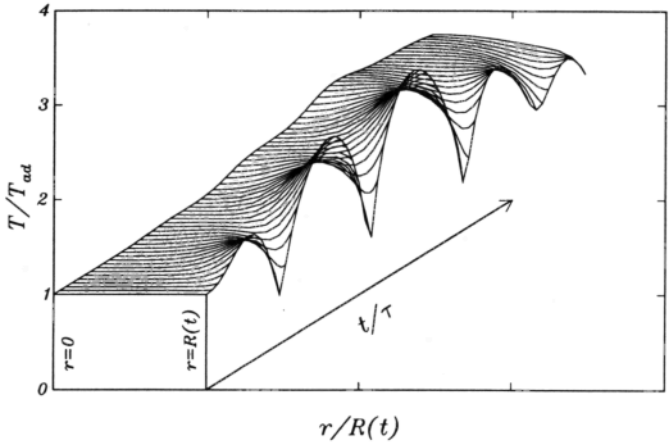

FIG. 10. Space-time plot of the gas temperature divided by the adiabatic value (12) during the first five cycles of the case $\omega/\omega_0 = 1$ of Figs. 3 and 4.

complex. In the first place, the distribution is often nonmontonic and such that even the direction of the heat exchange would be judged incorrectly by considering only the difference between the core and the wall temperatures. Second, the region of appreciably nonuniform temperature extends over at least 30% of the radius, which is indeed a number of the order of the estimated thermal boundary layer thickness $D^{1/2}$ for the cases considered here, but can hardly be considered small in the case of a sphere for which it contains 66% of the total volume. An interesting feature of these figures is also the rapidity with which the core temperature increases above the adiabatic value during the initial expansion phase.

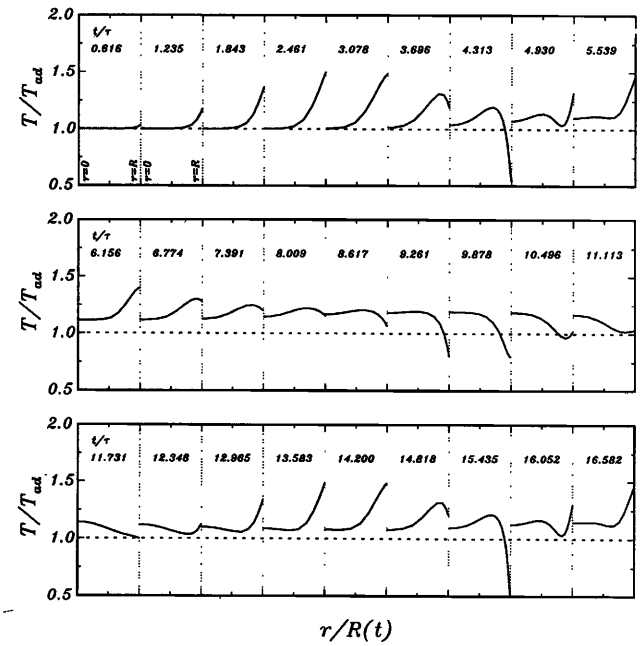

FIG. 11. Temperature distribution inside the bubble of Fig. 1 at 27 equally spaced instants during the first three cycles. The quantity plotted is the actual temperature divided by the adiabatic value (12).

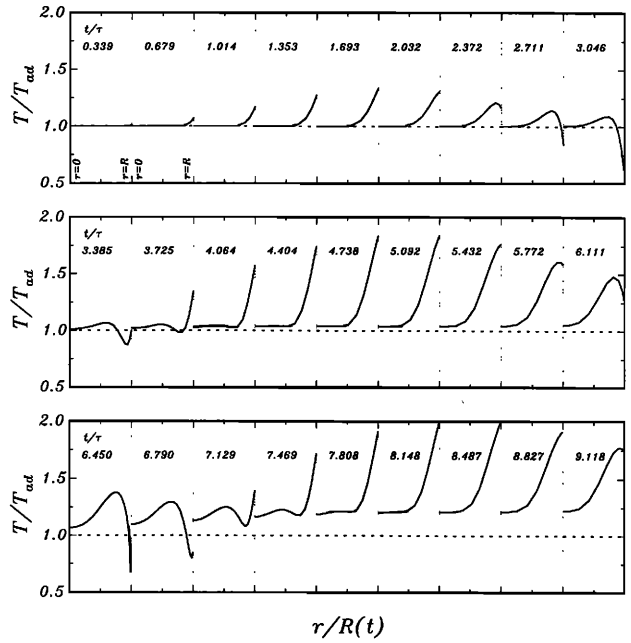

FIG. 12. Temperature distribution inside the bubble of Fig. 3 at 27 equally spaced instants during the first three cycles. The quantity plotted is the actual temperature divided by the adiabatic value (12).

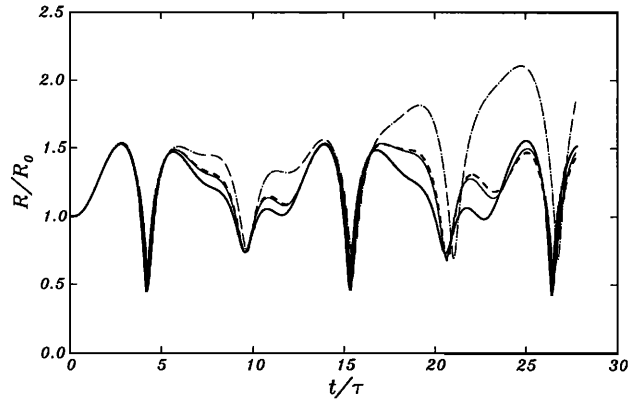

FIG. 13. Comparison of the complete model (thick solid line), the implicit nearly adiabatic approximations (3) (thin solid line) and (7) (thick dashes), and the explicit one (15) (dash-and-dotted line) during the first five cycles of Fig. 1.

V. ADDITIONAL COMMENTS

Before closing, the following additional comments on our results may be of some interest.

Since it has been found that the approximation is valid initially, we examine in greater detail the first few cycles. For small times one might be tempted to use the lower-order estimate $p_* = R_*^{-3\gamma}$ in the integrals in (3) and (4) to obtain (to the same formal order of accuracy) the *explicit* relations

$$p_* R_*^{3\gamma} = 1 + \frac{3\gamma}{4\pi}\left(\frac{D}{\pi}\right)^{1/2} \times \int_0^{\theta_*} [R_*^{3(\gamma-1)}(\theta_* - \eta_*) - 1]\eta_*^{-1/2}\, d\eta_*, \tag{15}$$

$$\theta_* = (4\pi)^2 \int_0^{t'_*} R_*^{4-3\gamma}(t'_*)\, dt'_*. \tag{16}$$

For the case of Fig. 1, we compare in Fig. 13 the two implicit nearly adiabatic approximations (3) (thin solid line) and (7) (thick dashes) with the complete model (thick solid line) and the explicit nearly adiabatic approximation (15), (16) (dash-and-dotted line). The four lines are all very close for the first cycle. The explicit approximation however deteriorates very quickly after that and already shows signs of transition at the 4th–5th cycle. The implicit approximations are very close over the time interval of this figure, although that of Eq. (3) is found to cause a slightly slower accumulation of the error because it predicts the transition to occur about five cycles later than Eq. (7).

We can understand this result if, with an obvious notation, we write for the moment Eq. (7) in the form

$$p_*^{1/\gamma} R_*^3 = 1 + \sqrt{D}\, Q, \tag{17}$$

and raise to the power γ to compare with (3) to find

$$p_* R_*^{3\gamma} = 1 + \sqrt{D}\,\gamma Q + \tfrac{1}{2}\gamma(\gamma - 1) D\, Q^2 + \cdots. \tag{18}$$

The use of (3) in place of (7) is therefore approximately equivalent to dropping the $O(D)$ term in this equation, which is clearly positive definite. For the same [to $O(1)$] pressure-time history, this would then result in a smaller radius and therefore a somewhat smaller error.

It is found numerically that the mass error of the nearly adiabatic approximation is reversible after the forcing is stopped. In other words, if the oscillations are calculated for some time and then the forcing ϵ is set to 0, the motion becomes a strongly damped oscillation around a slowly declining average radius that goes back to the original value 1. Analytically this can be explained by noting that, after the oscillations have essentially subsided, $p_* \sim 1$ so that the integrand of (7) effectively vanishes. From that point on the upper limit of the integral remains therefore fixed and the correction to the adiabatic law decays approximately as $t^{-1/2}$.

VI. CONCLUSIONS

We have examined the accuracy of the nearly-adiabatic approximation in two ways. One is a consistency check of the results, which shows that the approximation violates conservation of mass. The second one is the comparison of the bubble behavior predicted by the approximation with that given by a more complete model which contains it in a suitable limit. The disappointing finding has been that the approximation converges very slowly in the sense that the perturbation parameter D on the smallness of which it relies must be very small indeed for it to be accurate. For the cases examined by Miksis and Ting, in which D is of the order of 0.01, the error due to the neglect of higher-order terms very quickly accumulates and causes the approximation to fail after a short time. While this error manifests itself in a spurious increase of the gas mass, it is really caused by the failure of the approximation to capture the complex spatial and temporal behavior of the temperature field of the gas.

From the results shown in Figs. 10 and 11, it can be estimated that the gas temperature conforms with that as-

sumed in the approximation only for about the first half-cycle, during which it is monotonic in space with a core value well predicted by the adiabatic law. Since the bubble radius depends essentially on a two-fold time-integral of the pressure, the calculated $R(t)$ curve is close to that given by the complete model for a somewhat longer time, of the order of one cycle for the case of Figs. 1 and 11 and of the order of three cycles for that of Figs. 3 and 12.

Thus, in conclusion, we find that the nearly adiabatic approximation, beyond its remarkable conceptual significance, is probably not a practically useful tool for most applications.

ACKNOWLEDGMENTS

The authors are grateful to Professor M. J. Miksis for his careful comments and constructive criticisms of earlier versions of this paper. This study has been supported by the National Science Foundation under Grant No. CBT-8918144.

[1]M. J. Miksis and L. Ting, J. Acoust. Soc.Am. **76**, 897 (1984).
[2]M. J. Miksis and L. Ting, J. Acoust. Soc. Am. **81**, 1331 (1987).
[3]A. Prosperetti, J. Fluid Mech. **222**, 587 (1991).
[4]A. Prosperetti, L. A. Crum, and K. W. Commander, J. Acoust. Soc. Am. **83**, 502 (1988).
[5]V. Kamath and A. Prosperetti, J. Acoust. Soc. Am. **85**, 1538 (1989).
[6]C. W. Gear, *Numerical Initial-Value Problems in Ordinary Differential Equations* (Prentice-Hall, Englewood Cliffs, NJ, 1971).
[7]R. Piessens, E. deDoncker-Kapenga, C. W. Uberhuber, and D. K. Kahaner, *QUADPACK* (Springer-Verlag, New York, 1983).
[8]W. Lauterborn, J. Acoust. Soc. Am. **59**, 283 (1976).
[9]A. Prosperetti, J. Acoust. Soc. Am. **56**, 878 (1974).
[10]L. G. Tkachev and V. D. Shestakov, Sov. Phys. Acoust. **18**, 362 (1973).
[11]T. Wang, J. Acoust. Soc. Am. **56**, 1131 (1974).
[12]N. S. Khabeev, Sov. Phys. Acoust. **21**, 501 (1976).
[13]V. A. Akulichev, V. N. Alekseev, and V. P. Yushin, Sov. Phys. Acoust. **25**, 453 (1979).
[14]V. Kamath, A. Prosperetti, and F. Egolfopoulos, "A Theoretical Study of Sonoluminescence," J. Acoust. Soc. Am. (submitted).
[15]D. Y. Hsieh and M. S. Plesset, J. Acoust. Soc. Am. **33**, 206 (1961).